PHOTOSYNTHETICA
International Journal for Photosynthesis Research

DOI 10.32615/ps.2020.076 PHOTOSYNTHETICA 59 (1): 37-48, 2021

Chlorophyll retention caused by *STAY-GREEN* (*SGR*) gene mutation enhances photosynthetic efficiency and yield in soybean hybrid Z1

P. WANG*, S.Y. HOU*, H.W. WEN*, Q.Z. WANG**, and G.Q. LI*,+

*College of Agriculture, Shanxi Agricultural University, Taigu, 030801 Shanxi, China**
*College of Grassland Agriculture, Northwest A&F University, Yangling, 712100 Shaanxi, China***

Abstract

To study the effect of a stay-green mutation on photosynthetic efficiency in hybrid offspring of soybean (*Glycine max* [L.] Merr.), the parameters of photosynthesis and chlorophyll (Chl) fluorescence were compared between a new stay-green variety Jinda Zhilv No. 1 (Z1) and one of its parents Jinda No. 74 (JD74). During leaf natural senescence, the Chl degradation attenuated in Z1. The net photosynthetic rate, stomatal conductance, and transpiration rate were consistently higher in Z1 than that in JD74 after flowering. The decreases of maximum photochemical efficiency of PSII, actual photochemical efficiency of PSII, and photochemical quenching coefficient were greater in JD74 than in Z1. Transcriptional levels of most genes involved in photosystems were much higher in Z1. All these effectively contributed to maintained photosystem stability and enhanced photosynthetic efficiency and yield in Z1. We also revealed that the *STAY-GREEN* gene mutation was responsible for inhibiting Chl degradation in Z1.

Keywords: chlorophyll degradation; chlorophyll fluorescence; gene expression; photosynthetic rate; stay-green mutation.

Introduction

Chlorophyll (Chl) degradation is generally considered as the most obvious characteristic of leaf senescence, which results in leaf yellowing and decreased photosynthetic efficiency. Normally, Chl interacts with pigment-binding proteins of thylakoid membranes to form protein complexes, because free Chl is phototoxic. Once dissociated from the protein complex, it must be degraded as soon as possible (Pružinská *et al.* 2007). Chl is eventually converted to colorless breakdown products in a multi-step catabolic pathway by Chl catabolic enzymes (CCEs) (Sakuraba *et al.* 2014).

The stay-green trait in various plants generally refers to the retention of leaf green color during senescence and even after death (Kusaba *et al.* 2013). Stay-green mutants are of five types and further divided into functional and nonfunctional types (Thomas and Howarth 2000). Some functional stay-green mutants can maintain a stable photosynthetic activity and may have a better yield than that of their wild-type (WT) (Spano *et al.* 2003, Zheng *et al.* 2009), such as rice (*Oryza sativa*) *SNU-SG1* (Yoo *et al.*

Highlights

- *SGR* gene mutation results in Chl retention in soybean hybrid Z1
- Z1 plants show enhanced photosynthetic efficiency
- The photosynthetic apparatus of Z1 is less damaged during leaf senescence

Received 26 June 2020
Accepted 30 October 2020
Published online 18 December 2020

+Corresponding author
e-mail: li-gui-quan@126.com, 61901623@qq.com

Abbreviations: CCEs – Chl catabolic enzymes; Chl – chlorophyll; C_i – intercellular CO_2 concentration; E – transpiration rate; F_0 – minimal fluorescence yield of the dark-adapted state; F_m – maximal fluorescence yield of the dark-adapted state; FM – fresh mass; F_v/F_m – maximum photochemical efficiency of PSII; g_s – stomatal conductance; NPQ – nonphotochemical quenching; P_N – net photosynthetic rate; q_P – photochemical quenching coefficient; WT – wild type; Φ_{PSII} – actual photochemical efficiency of PSII.

Acknowledgments: This work was supported by the European Union's Horizon 2020 Program for Research & Innovation (grant No. 727312), the Ministry of Science and Technology of the People's Republic of China (Key projects for intergovernmental cooperation in science and technology innovation, grant No. 2017YFE0111000). We would like to thank *Editage* (www.editage.cn) for English language editing.

Conflict of interest: The authors declare that they have no conflict of interest.

2007), maize (*Zea mays*) *FS854* (Zheng *et al.* 2009), and wheat (*Triticum aestivum*) *xN901* (Gong *et al.* 2005). *STAY-GREEN* (*SGR*) gene mutation is responsible for the stay-green phenotype in various plant species (Park *et al.* 2007, Fang *et al.* 2014). Contrary to CCEs, SGR protein is not directly involved in the biochemical pathways of Chl degradation, and specifically interacts with the LHCII, resulting in Chl dissociation from complex proteins, and then enters the catabolic pathway (Park *et al.* 2007). Thus, it is a key regulator functioning in Chl degradation. In addition, SGR protein possibly recruits all six known CCEs to form a multiprotein complex of SGR–LHCII–CCEs for Chl degradation during senescence (Sakuraba *et al.* 2013).

Previous studies have shown that the net photosynthetic rate (P_N) of stay-green mutants decreased later and stayed significantly higher than that of their WT or parents during senescence (Spano *et al.* 2003, Tian *et al.* 2012, Fang *et al.* 2014, Wang *et al.* 2016). Photosynthesis depends on the function of the light-harvesting and electron transport systems within the chloroplasts which is indicated by the photochemical efficiency, measured as the Chl fluorescence (Spano *et al.* 2003). Both maximum photochemical efficiency of PSII (F_v/F_m) and actual photochemical efficiency of PSII (Φ_{PSII}) represent a measure of the functional status of PSII. In durum wheat, the F_v/F_m ratio decreased progressively in flag leaves after flowering, but much earlier in the parent than in the stay-green mutants (Spano *et al.* 2003). Tian *et al.* (2013) also reported that Φ_{PSII} and F_v/F_m decreased significantly under drought stress, while those decreases in *tasg1* wheat stay-green mutant were attenuated compared to the WT. However, there are few reports on the application of stay-green mutants in soybean breeding and the effects of stay-green mutation on photosynthetic physiology and yield of soybean.

We previously found a natural soybean stay-green mutant in the field, whose leaves remained green and showed no signs of yellowing during leaf senescence (even after abscission). However, its agronomic traits and yield performance are poor because of the genetic background. To make use of the advantage of stay-green mutation, we hybridized this mutant with a high-yield cultivar Jinda No. 74 (JD74), and bred a new stay-green variety, Jinda Zhilv No. 1 (Z1), which derived from a stay-green hybrid line after seven years of self-crossing homozygosity. The new stay-green variety Z1 has obvious hybridization advantages, which not only has the stay-green phenotype, but also the yield performance greater than that of JD74.

Hence, the main aim of this study was to understand the effects of stay-green mutation on photosynthetic efficiency in hybrid offspring of soybean, with a special focus on Chl fluorescence parameters and the transcriptional levels of photosystem-related genes. Furthermore, we also aimed to identify whether the cause of the stay-green mutation in our material is consistent with a previous study (Fang *et al.* 2014) and is due to the *SGR* gene mutation. The study expects to provide important information regarding the effect of stay-green mutation on photosynthetic capacity in hybrid offspring of soybean, and will be helpful in the application of stay-green mutants and *SGR* gene in soybean breeding and germplasm innovation.

Materials and methods

Plant materials: The new soybean variety Jinda Zhilv No. 1 (Z1), a typical leaf stay-green variety, was hybridized by a natural stay-green mutant and common cultivar Jinda No. 74 (JD74). Z1 plants exhibit an obvious stay-green phenotype; leaves show no yellowing during senescence and the seed coat is green in color. One of its parents, JD74, was chosen as the control.

Growth conditions: The Z1 and JD74 plants were grown in an experimental field of Shanxi Agricultural University, Taigu, China, in 2017 and 2018. In this field experiment, three replicate plots were planted for both varieties, a total of six 12-m^2 interspersed plots were established by random block design. Six rows for each plot, with a width of 2.5 m and a length of 6 m. Conventional agricultural management was maintained during the whole growth and development of soybeans, with timely intertilling and weeding. In anthesis, plants with the same growth trend and flowering on the same day were selected for listing and marking. Thereafter, the fully expanded functional leaves of the labeled plants were selected every 7 d. The samples were quickly frozen in liquid nitrogen, and then stored at –80°C for later use to determine various physiological parameters and analyze related gene expression (*see* below).

Yield appraisal: In 2018 and 2019, the ecological experiments were carried out at multiple sites. Each soybean material was harvested individually, and the important yield-related traits, including the mass per 100 seeds, the seed mass per plant, and seed number per plant were tested in the laboratory.

Chl content: Total Chl was extracted from leaves (approximately 0.1 g fresh mass) using 20 ml of ice-cold 80% acetone, and the absorbance was measured using a spectrophotometer (*UV-1200*, *MAPADA*, China) at 645, 663, and 470 nm (Porra *et al.* 1989).

Photosynthetic rate and Chl fluorescence: Photosynthetic rate-related parameters and Chl fluorescence parameters were measured using the portable photosynthesis system (*Li-6400*, *LI-COR*, USA). For net photosynthetic rate, five representative functional leaves were measured from 09:00 to 12:00 h, under a fixed LED light source [1,500 μmol(photon) m^{-2} s^{-1}] at 25°C, each repeated three times. Then, F_v/F_m, F_0, and F_m of PSII were measured from 14:00–16:00 h, after leaves were dark-adapted for 30 min wrapped in aluminum foil. The measurement method refers to the operating manual of the instrument.

DNA isolation, PCR, and sequencing: Genomic DNA isolation was performed using a *Plant Genomic DNA* kit (*Cowin Biotech Ltd.*, China). PCR amplification was segmented using *TaKaRa LA Taq* (*RR02MQ*) referring to the manual. Primers used in this study, in reference to a

previous study (Fang *et al.* 2014), are listed in Table 1S (*supplement*). The amplification products were detected using 1% agar-gel electrophoresis and then delivered to *Beijing Langfan Gene Technology Co.*, *Ltd.* for sequencing. Gene sequence analysis was compared with Williams 82 genomic sequence.

Gene expression analysis: Total RNA was extracted from leaves of five individual plants of each variety, using a *TRIzol* kit in accordance with the user manual. Samples of 2 μg of total RNA were reverse-transcribed using the *FastQuant RT* kit (*Tiangen Biotech*., China) after treatment with *DNase I* (*Takara*) to remove contaminating genomic DNA. Real-time quantitative PCR analysis was performed using a *SYBR Green I PCR* kit (*Takara*), with *His2* as a reference, repeated three times. Specific primers were designed using the online tools provided by the National Center for Biotechnology Information (NCBI) (Table 2S, *supplement*).

Statistical analysis: The obtained data were analyzed using *IBM SPSS Statistics 20*. Significant differences between the means (average of three replicates at least) among soybean varieties were compared using *Duncan*'s multiple range tests at $P<0.05$ levels. Figures were prepared using *GraphPad Prism 7*.

Results

Phenotype and yield-related traits: In both varieties, the total Chl content initially increased and then decreased gradually from anthesis to maturity, and the decrease was slower in Z1 from pod filling (29 d after flowering) (Fig. 1*A*). Compared to anthesis, the total Chl content

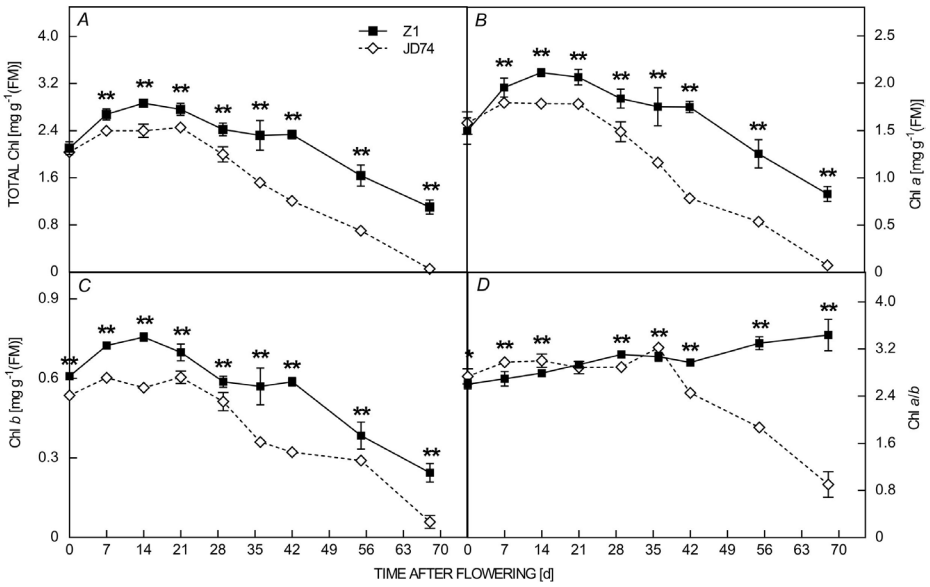

Fig. 1. Changes of total Chl content (*A*), Chl *a* content (*B*), Chl *b* content (*C*), and Chl *a*/*b* ratio (*D*) in two soybean varieties (Z1 and JD74) after flowering. The error bars indicate SD (n = 3). $^{*}P<0.05$; $^{**}P<0.01$. The leaf color comparison of Z1 (*left*) and JD74 (*right*) at the late stage of maturity in the field (*E*).

was 65.6 and 22.1% lower in JD74 and Z1 leaves at 55 d after flowering, respectively. Moreover, Chl was almost fully degraded in leaves of JD74 at the end of maturity but remained at a relatively high content in Z1 leaves. We observed obviously that the leaf color of Z1 remained green at the late maturity stage in the field, while it turned yellow in JD74 (Fig. 1*E*). Chl *a* and Chl *b* variation was basically the same as that of total Chl (Fig. 1*B*,*C*). Regarding the Chl *a*/*b* ratio (Fig. 1*D*), Z1 remained at approximately 3.0 from anthesis to maturity. However, in JD74, the Chl *a*/*b* ratio decreased after 36 d after flowering and was only 0.9 at the end of maturity mainly owing to the more rapid Chl *a* degradation. Senescence had no obvious effect on the Chl *a*/*b* ratio of Z1 stay-green variety, indicating that the degradation rate of Chl *a* and Chl *b* were almost similar. Therefore, we hypothesized that the Z1 stay-green phenotype was not caused by the mutation of enzymes related to Chl degradation, but the mutation of the *SGR* gene.

In addition, as the yield-related traits comparisons showed (Table 1), though the mass per 100 seeds was lower in Z1, the seed mass per plant, and the seed number per plant were higher in Z1 than that in JD74. Thus, the yield performance of Z1 was greater than that of JD74.

Photosynthetic rate-related parameters: As shown in Fig. 2*A*, P_N decreased to the minimum at the early stage of podding (14 d after flowering) and peaked at filling stage (42 d after flowering) in both soybean varieties. Meanwhile, it was significantly higher in Z1 than that in JD74 after flowering, especially from 21 to 55 d after flowering. The stomatal conductance (g_s) of JD74 decreased rapidly after 7 d after flowering, whereas it decreased after 36 d after flowering in Z1 (Fig. 2*B*). Notably, during the podding stage (approximately 21–42 d after flowering), g_s was much higher in Z1 than that in JD74. Similar variations in the transpiration rate (*E*) were observed after flowering (Fig. 2*D*). It was lower in JD74 than that in Z1 and

Table 1. The yield-related traits comparisons in two soybean varieties (Z1 and JD74). Each soybean material was planted at multiple sites for an ecological experiment. In 2018, three replicate 12-m^2 plots were planted for both varieties at each location. In 2019, 300-m^2 plots were planted for both varieties at each location. Values are means ± SD (n = 6).

Year	Variety	100-seed mass [g]	Seed mass per plant [g]	Seed number per plant	Plot yield [kg 12 m^{-2}]	Plot yield [kg 300 m^{-2}]
2018	Z1	21.50 ± 1.78	33.82 ± 7.78	153.62 ± 37.90	3.99 ± 1.13	-
	JD74	23.15 ± 2.46	31.51 ± 7.63	140.44 ± 31.12	3.66 ± 1.11	-
2019	Z1	20.72 ± 1.20	26.98 ± 5.33	136.70 ± 26.23	-	85.57 ± 13.17
	JD74	22.42 ± 1.48	25.16 ± 5.21	116.86 ± 22.49	-	79.35 ± 12.56

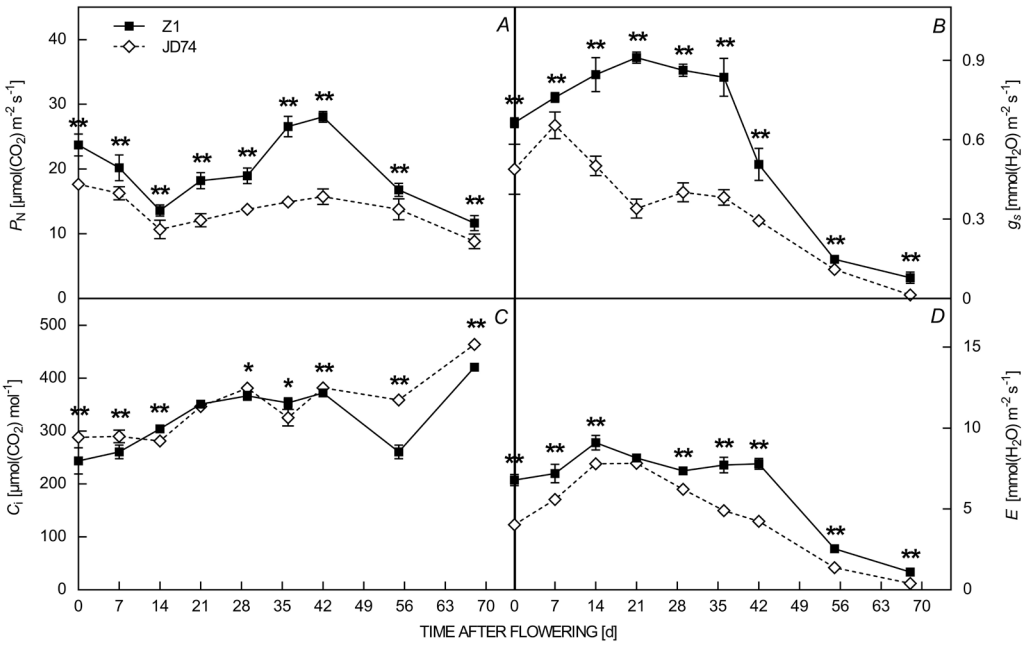

Fig. 2. Changes of photosynthetic rate-related parameters in two soybean varieties (Z1 and JD74) after flowering. Net photosynthetic rate (P_N) (*A*), stomatal conductance (g_s) (*B*), intercellular CO_2 concentration (C_i) (*C*), and transpiration rate (*E*) (*D*). The error bars indicate SD (n = 5). $^*P<0.05$; $^{**}P<0.01$.

decreased much earlier. Intercellular CO_2 concentration (C_i) increased gradually in both varieties (Fig. 2*C*). However, in Z1, C_i decreased suddenly in the late period of seed filling and increased thereafter.

Chl fluorescence parameters: Minimal fluorescence yield of the dark-adapted state (F_0) and maximal fluorescence yield of the dark-adapted state (F_m) values are two important indices that indicate the damage and electron transport efficiency of PSII during leaf senescence, respectively. As shown in Fig. 3*A*, F_0 increased significantly in JD74 but increased only slightly in Z1 after 55 d after flowering. In addition, no significant difference in F_m was observed between JD74 and Z1 from 0 to 42 d after flowering but it decreased faster in JD74 than in Z1 from 42 to 55 d after flowering (Fig. 3*B*).

F_v/F_m, often used to measure the potential activity of PSII, is known as the energy capture efficiency of opened PSII reaction centers (Hao *et al*. 2011). Under stress-free conditions, its value is generally close to 0.83 (Kalaji *et al.* 2012). As shown in Fig. 3*C*, F_v/F_m decreased more quickly in JD74 after 42 d after flowering and significantly lower than that in Z1. Φ_{PSII} is the proportion of total excitation energy entering PSII used in the photochemical pathway, it represents the photosynthetic capacity. As shown in Fig. 3*D*, Φ_{PSII} decreased rapidly from the early stage of filling (29 d after flowering) in both soybean genotypes but the value of this parameter was significantly higher in Z1 than that in JD74.

Photochemical quenching coefficient (q_P) and non-photochemical quenching (NPQ) reflect the proportion of light energy absorbed by the PSII antenna pigment for photochemical electron transfer or thermal radiation, respectively. The larger the q_P, the greater the electron transfer activity of PSII. NPQ is a self-protection mechanism of photosynthetic apparatus against damage from excess light energy (Elsheery *et al.* 2020a). As shown in Fig. 3*E*,*F*, both q_P and NPQ were reduced during later senescence. The value of q_P was significantly higher in Z1 than that in JD74 after 29 d after flowering, whereas the NPQ of JD74 was significantly higher than that of Z1 after 36 d after flowering.

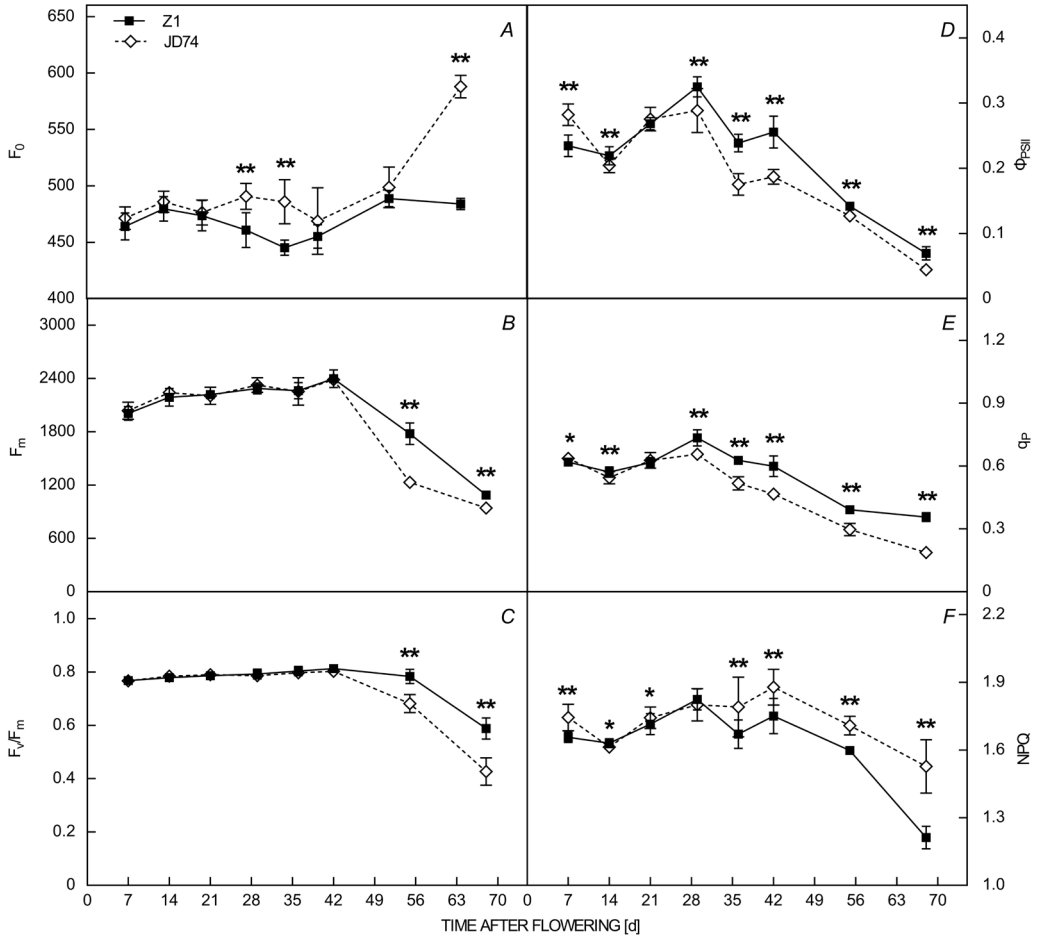

Fig. 3. Changes of chlorophyll fluorescence parameters in two soybean varieties (Z1 and JD74). Minimal fluorescence yield of the dark-adapted state (F_0) (*A*), maximal fluorescence yield of the dark-adapted state (F_m) (*B*), maximum photochemical efficiency of PSII (F_v/F_m) (*C*), actual photochemical efficiency of PSII (Φ_{PSII}) (*D*), photochemical quenching coefficient (q_P) (*E*), and nonphotochemical quenching (NPQ) (*F*). The error bars indicate SD (n = 5). $^{*}P<0.05$; $^{**}P<0.01$.

Transcriptional levels of genes involved in PSI and PSII: In higher plants, PSI consists of the reaction center protein complexes and outer antenna protein. P700A and P700B, as the core proteins of the reaction center, are encoded by *PsaA* and *PsaB*, respectively. Antenna proteins are complexes of Chl *a*/*b*-binding proteins encoded by the *Lhca* gene family. As shown in Fig. 4*A*, the relative mRNA level of *PsaA* decreased to the minimum level at 14 d after flowering in both soybean varieties, then was upregulated with senescence. Meanwhile, it was significantly higher in Z1 than that in JD74, except for some limited tested time points. On the contrary, *PsaB* gene was repressed after 14 d after flowering (Fig. 4*B*). Expression levels of genes, including *Lhca1*, *Lhca2*, *Lhca3*, *Lhca4*, and *Lhca6* of Z1, were significantly higher than those of JD74 at anthesis (0 d after flowering) (Fig. 4). As shown in Fig. 4*C–H*, the expression of six *Lhca* family genes was divided into three modes. For example, *Lhca1* and *Lhca4* were significantly repressed after 14 d after flowering. Expression of *Lhca2* and *Lhca3* was upregulated after 29 d after flowering. Expression of *Lhca5* and *Lhca6* was repressed after flowering all the time.

As revealed by qRT-PCR (Fig. 5*A–D*), the dynamic expression patterns of genes encoding the PSII core protein, including *PsbA*, *PsbB*, *PsbC*, and *PsbD*, showed the same trend in both varieties. The expression level of these genes was significantly higher in Z1 than that in JD74 at most of the tested time points. The relative mRNA levels of all six *Lhcb* genes tested were significantly greater in Z1 than in JD74 at anthesis (Fig. 5*E*). As shown in Fig. 5*F–K*, the expression patterns of six *Lhcb* isogenes were similar in both varieties after flowering, which were

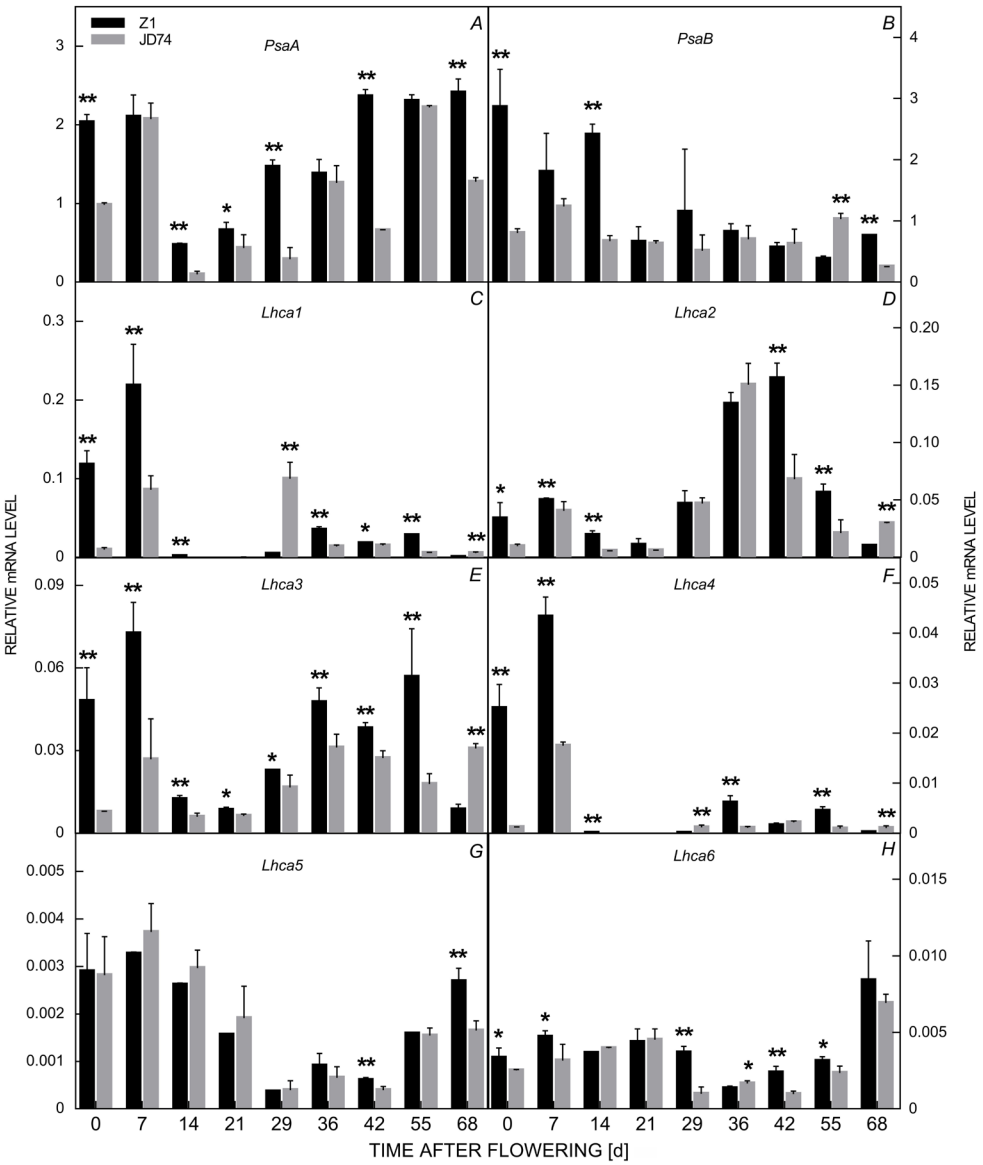

Fig. 4. Changes of relative mRNA levels of genes involved in PSI in soybean varieties JD74 and Z1 after flowering. *PsaA* (*A*), *PsaB* (*B*), *Lhca1* (*C*), *Lhca2* (*D*), *Lhca3* (*E*), *Lhca4* (*F*), *Lhca5* (*G*), and *Lhca6* (*H*). The error bars indicate SD ($n = 3$). $^{*}P<0.05$; $^{**}P<0.01$.

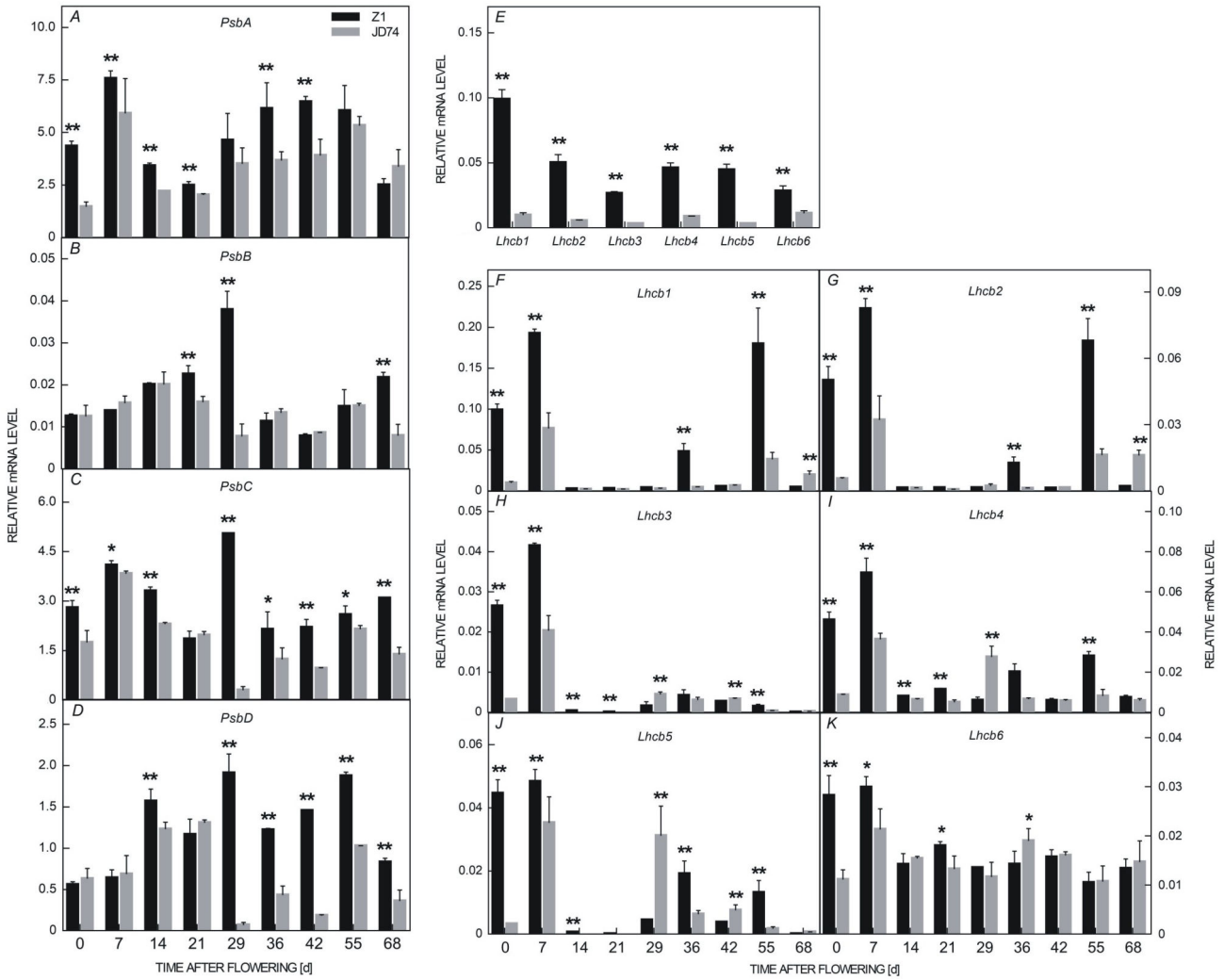

Fig. 5. Changes of relative mRNA levels of genes involved in PSII in soybean varieties JD74 and Z1 after flowering. *PsbA* (*A*), *PsbB* (*B*), *PsbC* (*C*), *PsbD* (*D*). The expression levels of six *Lhcb* isogenes at anthesis (*E*). *Lhcb1* (*F*), *Lhcb2* (*G*), *Lhcb3* (*H*), *Lhcb4* (*I*), *Lhcb5* (*J*), and *Lhcb6* (*K*). The error bars indicate SD (n = 3). $^{*}P<0.05$; $^{**}P<0.01$.

upregulated at 7 d after flowering with higher expression in Z1 than that in JD74. Then, they were inhibited at an extremely low expression level except for several tested points. For example, *Lhcb1*, *Lhcb2*, *Lhcb3*, *Lhcb4*, *Lhcb5* were upregulated at 36 and 55 d after flowering in Z1 and significantly higher than in JD74; *Lhcb3*, *Lhcb4*, and *Lhcb5* of JD74 were upregulated at 29 d after flowering and significantly higher than those of Z1.

***SGR1* gene sequence variation analysis**: To validate the previous hypothesis that the Z1 stay-green phenotype is caused by an *SGR* mutation, we amplified the target genes *SGR1/2* by PCR. The amplification product of three *SGR1* fragments was of the same size in both varieties, whereas the third *SGR2* segment of Z1 was > 10 kb (Fig. 6*A*), suggesting a large fragment insertion in the gene.

We obtained the complete genome sequences of *SGR1* in both varieties but failed to determine the *SGR2* gene sequences of Z1 owing to the complex structure. As shown in the gene structure analysis (Fig. 6*B*), both in JD74 and Williams 82, the *SGR1* gene had four exons, containing 129, 174, 168, and 345 bp, encoding a total of 271 amino acids. However, the second exon of Z1 was significantly shortened with 126 bp missing, encoding a truncated protein with only 229 amino acids. Further alignment between the genome and CDS sequence indicated that an incorrect alternative splicing site was generated owing to the single nucleotide deletion, which resulted in the inaccurate splice of the second exon (Fig. 6*C*). This resulted in 42 amino acids missing between the 60th and 101st amino acid of this protein (Fig. 7*A*). Results of the protein structure prediction showed that the Z1 SGR1 protein exhibited great changes in tertiary structure, such as an increased α-helix and a shortened irregular curl (Fig. 7*B*,*C*). Meanwhile, it lost the parts of the functional domain that were located between the 50th to 204th amino acid. Thus, it is possible that the Z1 stay-green variety already lost the main function of the SGR1 protein.

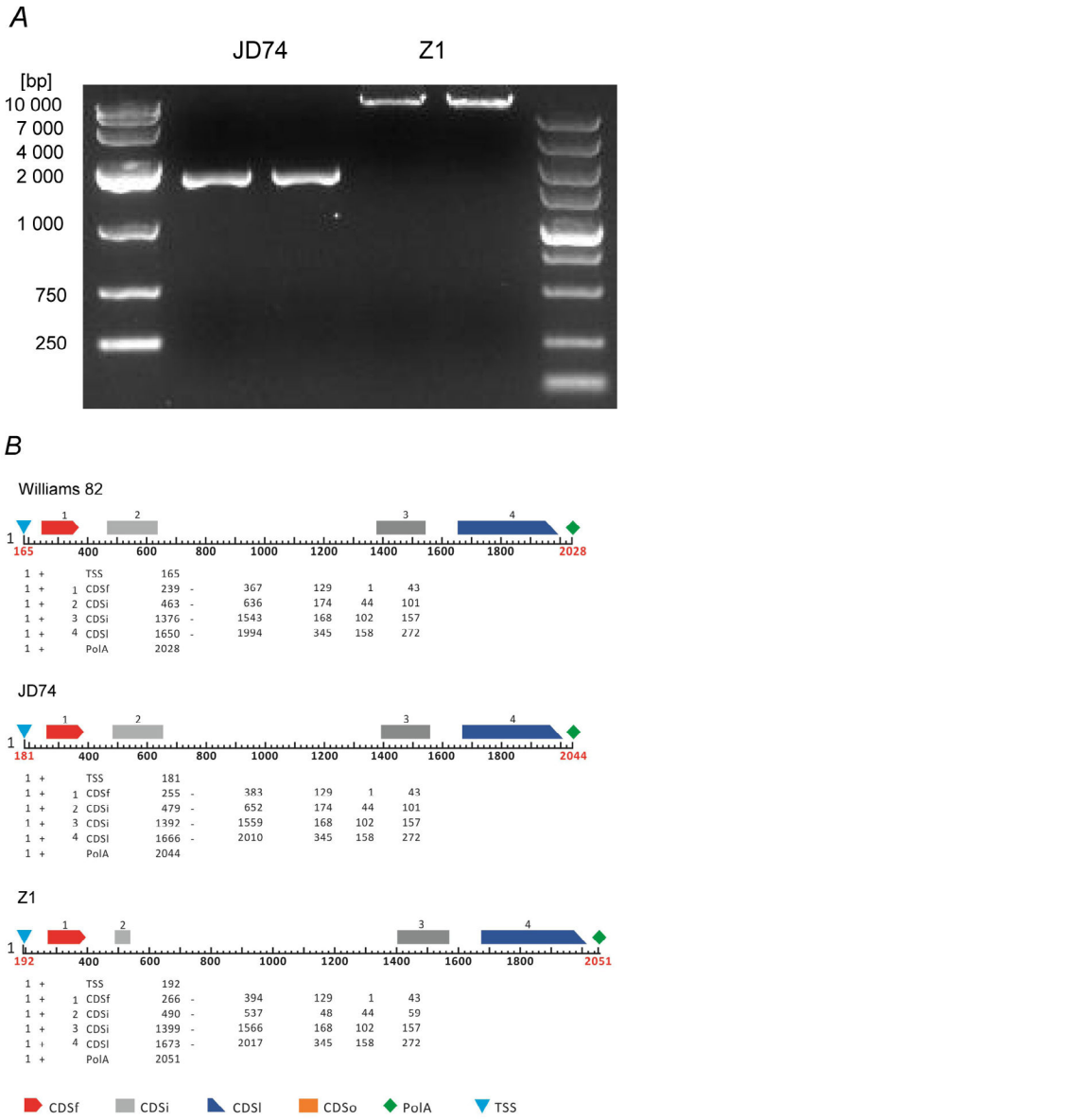

Fig. 6. Analysis of *SGR* gene structure. (*A*) Polymorphism of *SGR2-3* in soybean varieties Z1 and JD74. The amplification of the third *SGR2* segment in Z1 was > 10 kb, suggesting a large fragment of gene sequence was inserted. (*B*) *SGR1* gene structure of Williams 82, JD74, and Z1. The second exon of Z1 is significantly shortened with 126 nucleotides missing, resulting in the encoding of only 229 amino acids. (*C*) Alignment between the genome and CDS sequence in the second exon of *SGR1*. An incorrect variation splicing site was generated owing to the single nucleotide deletion (highlighted with *red* colour), which resulted in significantly shortened second exon of Z1 with 126 bp missing (indicated by *green*).

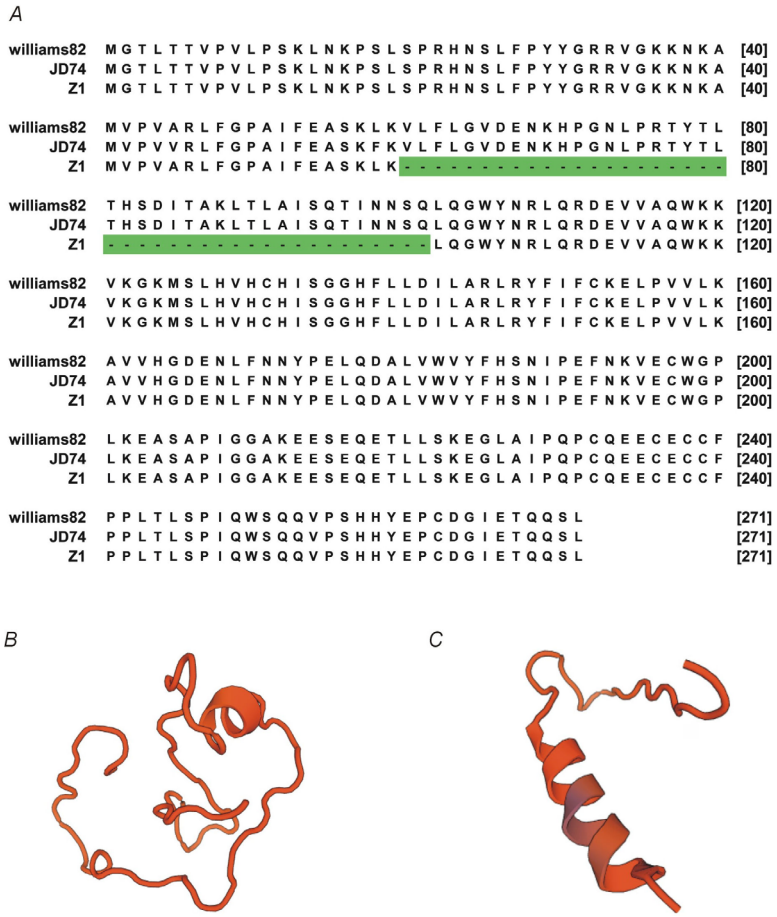

Fig. 7. Amino acid sequences and protein structure prediction of SGR1. (*A*) The amino acid sequences of SGR1 protein in Williams 82, JD74, and Z1. 42 amino acids between the 60th and 101th amino acid are missing in stay-green variety Z1, highlighted with green. (*B*,*C*) SGR1 protein structure prediction of JD74 and Z1. It exhibits a great change in tertiary structure owing to the mutation in Z1 (*C*), such as an increased α-helix and a shortened irregular curl.

Discussion

Retention of Chl contributes to enhanced photosynthetic efficiency in Z1

Chl degradation and leaf yellowing are typical characteristics during green plant senescence, which are usually obvious indicators of leaf senescence. The decrease in Chl concentration could induce a reduction in net photosynthetic rate (Elsheery *et al.* 2020b). Compared with JD74, Z1 plants exhibited marked leaf color retention, and the Chl content remained at a higher level until late maturity. Thus, the net photosynthetic rate of Z1 was significantly higher than that of JD74. In general, factors that limit photosynthesis can be divided into stomatal or nonstomatal ones (Dąbrowski *et al.* 2019). Ohashi *et al.* (2006) reported that stomatal closure leads to a decrease in leaf photosynthesis. Our results also proved that in leaf senescence, g_s decreased in both varieties, which might be responsible for the reduction of P_N. Similar phenomena were noticed for the transpiration rate. However, those parameters were significantly higher in Z1 than that in JD74, indicating that the stay-green phenotype in Z1 contributed to the enhancement of the photosynthetic activity, especially in podding and filling stages (approximately 14–42 d after flowering). Furthermore, declined C_i of Z1 in the late period of filling showed the enhancing of CO_2-use efficiency, which contributed to higher photosynthetic efficiency and delaying leaf senescence.

We further determined Chl fluorescence, which is a key measure of photosynthetic activity and performance (Baker 2008, Chen *et al.* 2019). F_0 represents the Chl fluorescence emission intensity of the fully opened chloroplast PSII reaction center (Dąbrowski *et al.* 2015). The increase in the F_0 parameter is explained by the loss of PSII reaction centers and their inactivation (Cui *et al.* 2006, Fu *et al.* 2012). F_m was detected when all reaction centers were fully closed (Dąbrowski *et al.* 2015), which reflects the situation of electron transfer. Thus, the higher value of F_0 in JD74 from 29 d after flowering suggested that its photosynthetic apparatus suffered more serious damage during leaf senescence and resulted in the reduction of electron transfer efficiency.

Maximum PSII efficiency, F_v/F_m, reflects the original optical energy conversion efficiency within PSII reaction centers, which is a reliable parameter to estimate the photochemical activity of PSII (Kalaji *et al.* 2012). Moreover, the F_v/F_m value is also an important indicator in plant stress physiology (Laxman *et al.* 2013, Sunoj *et al.* 2016); it decreases significantly during senescence or stress (Li *et al.* 2002, Wang *et al.* 2012, Elsheery *et al.* 2020b). Improved F_v/F_m demonstrates the amelioration capacity of maximum photochemical efficiency of PSII under stress (Elsheery *et al.* 2020a). Φ_{PSII}, the actual photochemical

quantum efficiency of PSII, reflects the ratio of total excitation energy of PSII in the photochemical pathway, which is an important indicator for the photosynthetic capacity of plants. Furthermore, q_P reflects the share of light energy absorbed by the PSII antenna protein for photochemical electron transfer. Our study revealed that all those three parameters decreased more rapidly in JD74 during leaf senescence and were significantly lower in JD74 than in Z1. This indicated that the photochemical efficiency of JD74 was lower than that of the stay-green variety Z1.

With lowered P_N and the photochemical efficiency during leaf senescence, the requirement for photosynthetic electrons decreases so that surplus radiant energy was generated (Elsheery and Cao 2008). Excess light energy can enhance the production of free oxygen radicals, which leads to peroxidation damage to cell membranes. NPQ reflects the portion of excess light energy dissipated by heat radiation, which is important to prevent photoinhibition or protect the photosystem from peroxidation damage (Elsheery and Cao 2008, Derks *et al.* 2015). It progressively increased under drought stress (Elsheery and Cao 2008) and different salinity levels (Elsheery *et al.* 2020b). However, in this work, the value of NPQ decreased after 42 d after flowering in both varieties. Indeed, there are two different modes of heat dissipation in plants. One relies on the xanthophyll cycle, named q_f, which is the primary mechanism for heat dissipation (Demmig-Adams and Adams 1996) and is located in the photosynthetic antenna system; the other is q_I, which is independent of the xanthophyll cycle and may be located in the PSII reaction center (Bukhov *et al.* 2001). It has been confirmed that parts of the PSII inactivated reaction center protein function in dissipating excess light energy (Krause 1988). It is generated in large quantities during senescence and used as energy storage to protect the neighboring active reaction center from damage caused by excess light energy (Lee *et al.* 2001). This implied that the mechanism of leaf heat dissipation varied during different degrees of senescence. In this study, the photochemical efficiency of JD74 was lower than that of Z1 and required more heat dissipation to avoid photosynthetic system damage under the same radiation. Therefore, the value of NPQ was much higher in JD74 after 36 d after flowering. With developing senescence, heat dissipation that is solely dependent on the xanthophyll cycle (q_f) was not sufficient to protect the photosynthetic apparatus from the damage caused by excess light energy. The heat dissipation was gradually transferred from the antenna system to the PSII reaction center, resulting in a decrease in the value of NPQ in both varieties.

Relationship between the photosynthetic efficiency and transcriptional level of genes involved in the photosystems

Photosystems (PSI and PSII) are pigment–protein complexes with multiple subunits, located in the thylakoid membrane of chloroplasts. Photosystems are involved in harvesting light energy, electron transfer, and transformation. Each has its reaction center protein and light-harvesting complex protein, encoded by *psa/b* and *Lhca/b* gene families, respectively (Derks *et al.* 2015). Their activities decrease gradually during senescence owing to considerable changes to the integrity and stability of thylakoid membrane proteins (Hashimoto *et al.* 1989). *Lhca* and *Lhcb* gene expression levels, as well as LHCI and LHCII stability, are of great importance for maintaining high photosynthetic activity (Standfuss *et al.* 2005, Sato *et al.* 2009). The degradation of D1 and D2 protein in PSII, which form the skeleton for the heterodimeric reaction center (Derks *et al.* 2015), could be accelerated by senescence or stress (Niyogi 1999). During incubation in the dark, the abundance of Chl-protein complexes decreased dramatically in the wild type, but in *d1d2* (*SGR1/SGR2*) mutant, the LHCP trimer, dimer, and monomer were still apparent (Fang *et al.* 2014). Tian *et al.* (2013) reported that the expression levels of *TaLhcb4* and *TaLhcb6* in the stay-green mutant *tasg1* were higher than that of the wild type, and it was also found that *tasg1* could maintain higher TaLhcb4 and TaLhcb6 protein levels under drought stress by protein immunization experiments.

In the present study, the transcriptional levels of most genes involved in PSI and PSII were all much higher in Z1 during anthesis to maturity. This indicated that the photosystem of the stay-green variety had a stronger ability to synthesize reactive center proteins, thereby increasing its integrity and stability during senescence. Meanwhile, most Chl molecules in Z1 failed to dissociate from the pigment–protein complex owing to the enhanced stability of pigment-binding proteins, which resulted in a decrease in Chl degradation and increased Chl retention. Interestingly, LhcI (*Lhca*) can be divided into two types of protein complexes, LhcI-680 and LhcI-730, using a detergent treatment. LhcI-680 is composed of Lhca2 and Lhca3, whereas LhcI-730 is composed of Lhca1 and Lhca4 (Park *et al.* 2007). The synergy of *Lhca* expression patterns in our study further confirmed these results; *Lhca1* and *Lhca4* were upregulated in early development, whereas *Lhca2* and *Lhca3* were upregulated in the middle and late stages. This revealed that members of the *Lhca* gene family cooperated in pairs to function in different plant developmental stages.

***SGR1/2* gene mutation responsible for the Z1 stay-green phenotype**

The higher plant *SGR* gene family is composed of multiple members, which can be classified into two subfamilies, *SGR* and *SGR-LIKE* (*SGRL*), strongly suggesting they function in chloroplast and possibly Chl metabolism (Sakuraba *et al.* 2014). For example, rice contains *OsSGR* and *OsSGRL* (Cha *et al.* 2002). Maize and *Arabidopsis* harbor three *SGR* homologous genes, namely *SGR1*, *SGR2*, and *SGRL* (Rong *et al.* 2013). Previous studies have shown that the mutation of *SGR* is responsible for the stay-green phenotype in many crops (Park *et al.* 2007).

There are five *SGR* homologs in the soybean genome, among which *GmSGR1* (*D1*) and *GmSGR2* (*D2*) belong to the *SGR* subfamily, and are two homologous copies

distributed on chromosome 1 and chromosome 11 (Fang *et al.* 2014); *GmSGR4* belongs to the *SGRL* subfamily; the other two genes, *GmSGR3a* and *GmSGR3b*, are presumed to be nonfunctional pseudogenes (Nakano *et al.* 2014). In the present study, we obtained the whole genome sequence of the stay-green variety *SGR1*, although it also contained four exons that were the same as JD74 and Williams 82, a wrong variable splice site GT-AG was formed in the second exon owing to the single base deletion, which resulted in a wrongly variable shear in mRNA and shortened 42 amino acids. The protein structure prediction showed that the missing part of these amino acids was located in the SGR1 protein critical function domain; thus, the single-base mutation of *SGR1* leads to weakening or losing the function of its coding protein, which caused Chl retention.

In conclusion, Z1 is a typical leaf stay-green variety caused by a double mutation of *SGR1* and *SGR2*. Compared with the JD74, the transcriptional levels of genes involved in LHCI and LHCII were much higher in Z1 and the photosynthetic apparatus of Z1 was less damaged during senescence, which contributed to the stability of PSI and PSII. Especially in the podding and filling stages, which are critical for soybean yield, the Chl content was much higher in Z1 than in JD74, which contributed to enhanced photosynthetic efficiency and determined a better performance of Z1 yield. This study is significant for the application of stay-green mutants and *SGR* genes in soybean breeding and germplasm innovation.

References

Baker N.R.: Chlorophyll fluorescence: a probe of photosynthesis *in vivo*. – Annu. Rev. Plant Biol. **59**: 89-113, 2008.

Bukhov N.G., Heber U., Wiese C., Shuvalov V.A.: Energy dissipation in photosynthesis: Does the quenching of chlorophyll fluorescence originate from antenna complexes of photosystem II or from the reaction center? – Planta **212**: 749-758, 2001.

Cha K.W., Lee Y.J., Koh H.J. *et al.*: Isolation, characterization, and mapping of the stay green mutant in rice. – Theor. Appl. Genet. **104**: 526-532, 2002.

Chen Y.E., Wu N., Zhang Z.W. *et al.*: Perspective of monitoring heavy metals by moss visible chlorophyll fluorescence parameters. – Front. Plant Sci. **10**: 35, 2019.

Cui X., Niu H., Wu J. *et al.*: Response of chlorophyll fluorescence to dynamic light in three alpine species differing in plant architecture. – Environ. Exp. Bot. **58**: 149-157, 2006.

Dąbrowski P., Baczewska-Dąbrowska A.H., Kalaji H.M. *et al.*: Exploration of chlorophyll *a* fluorescence and plant gas exchange parameters as indicators of drought tolerance in perennial ryegrass. – Sensors **19**: 2736, 2019.

Dąbrowski P., Pawluśkiewicz B., Baczewska A.H. *et al.*: Chlorophyll *a* fluorescence of perennial ryegrass (*Lolium perenne* L.) varieties under long term exposure to shade. – Zemdirbyste **102**: 305-312, 2015.

Demmig-Adams B., Adams III W.W.: The role of the xanthophylls cycle carotenoids in the protection of photosynthesis. – Trends Plant Sci. **1**: 21-26, 1996.

Derks A., Schaven K., Bruce D.: Diverse mechanisms for photoprotection in photosynthesis. Dynamic regulation of photosystem II excitation in response to rapid environmental change. – BBA-Bioenergetics **1847**: 468-485, 2015.

Elsheery N.I., Cao K.F.: Gas exchange, chlorophyll fluorescence, and osmotic adjustment in two mango cultivars under drought stress. – Acta Physiol. Plant. **30**: 769-777, 2008.

Elsheery N.I., Helaly M.N., Omar S.A. *et al.*: Physiological and molecular mechanisms of salinity tolerance in grafted cucumber. – S. Afr. J. Bot. **130**: 90-102, 2020b.

Elsheery N.I., Sunoj V.S.J., Wen Y. *et al.*: Foliar application of nanoparticles mitigates the chilling effect on photosynthesis and photoprotection in sugarcane. – Plant Physiol. Bioch. **149**: 50-60, 2020a.

Fang C., Li C.C., Li W.Y. *et al.*: Concerted evolution of *D1* and *D2* to regulate chlorophyll degradation in soybean. – Plant J. **77**: 700-712, 2014.

Fu W., Li P., Wu Y.: Effects of different light intensities on chlorophyll fluorescence characteristic and yield in lettuce. – Sci. Hortic.-Amsterdam **135**: 45-51, 2012.

Gong Y.H., Zhang J., Gao J.F. *et al.*: Slow export of photoassimilate from stay-green leaves during late grain-filling stage in hybrid winter wheat (*Triticum aestivum* L.). – J. Agron. Crop Sci. **191**: 292-299, 2005.

Hao X.Y., Han X., Li P. *et al.*: [Effects of elevated atmospheric CO_2 concentration on mung bean leaf photosynthesis and chlorophyll fluorescence parameters.] – Chin. J. Appl. Ecol. **22**: 2776-2780, 2011. [In Chinese] doi: 10.13287/j.1001-9332.2011.0390.

Hashimoto H., Kura-Hotta M., Katoh S.: Changes in protein content and in the structure and number of chloroplasts during leaf senescence in rice seedlings. – Plant Cell Physiol. **30**: 707-715, 1989.

Kalaji H.M., Goltsev V., Bosa K. *et al.*: Experimental *in vivo* measurement of light emission in plants: a perspective dedicated to David Walker. – Photosynth. Res. **114**: 69-96, 2012.

Krause G.H.: Photoinhibition of photosynthesis: An evaluation of damaging and protective mechanisms. – Physiol. Plantarum **74**: 566-574, 1988.

Kusaba M., Tanaka A., Tanaka R.: Stay green plants: What do they tell us about the molecular mechanism of leaf senescence. – Photosynth. Res. **117**: 221-234, 2013.

Laxman R.H., Srinivasa Rao N.K., Bhatt R.M. *et al.*: Response of tomato (*Lycopersicon esculentum* Mill.) genotypes to elevated temperature. – J. Agrometeorol. **15**: 38-44, 2013.

Lee Y.H., Hong Y.N., Chow W.S.: Photoinactivation of photosystem II complexes and photoprotection by non-functional neighbors in *Capsicum annuum* L. leaves. – Planta **212**: 332-342, 2001.

Li X., Jiao D.M., Liu Y.L., Huang X.Q.: Chlorophyll fluorescence and membrane lipid peroxidation in the flag leaves of different high yield rice variety at late stage of development under natural condition. – Acta Bot. Sin. **44**: 413-421, 2002.

Nakano M., Yamada T., Masuda Y. *et al.*: A green-cotyledon/stay-green mutant exemplifies the ancient whole-genome duplications in soybean. – Plant Cell Physiol. **55**: 1763-1771, 2014.

Niyogi K.K.: Photoprotection revisited: genetic and molecular approaches. – Annu. Rev. Plant Phys. **50**: 333-359, 1999.

Ohashi Y., Nakayama N., Saneoka H., Fujita K.: Effects of drought stress on photosynthetic gas exchange, chlorophyll fluorescence and stem diameter of soybean plants. – Biol. Plantarum **50**: 138-141, 2006.

Park S.Y., Yu J.W., Park J.S. *et al.*: The senescence-induced staygreen protein regulates chlorophyll degradation. – Plant Cell **19**: 1649-1664, 2007.

Porra R.J., Thompson W.A., Kriedemann P.E.: Determination of accurate extinction coefficients and simultaneous equations for assaying chlorophylls *a* and *b* extracted with four different

solvents: verification of the concentration of chlorophyll standards by atomic absorption spectroscopy. – BBA-Bioenergetics **975**: 384-394, 1989.
Pružinská A., Anders I., Aubry S. *et al.*: In vivo participation of red chlorophyll catabolite reductase in chlorophyll breakdown. – Plant Cell **19**: 369-387, 2007.
Rong H., Tang Y.Y., Zhang H. *et al.*: The *Stay-Green Rice like* (*SGRL*) gene regulates chlorophyll degradation in rice. – J. Plant Physiol. **170**: 1367-1373, 2013.
Sakuraba Y., Kim D., Kim Y.S. *et al.*: *Arabidopsis* STAYGREEN-LIKE (SGRL) promotes abiotic stress-induced leaf yellowing during vegetative growth. – FEBS Lett. **588**: 3830-3837, 2014.
Sakuraba Y., Kim Y.S., Yoo S.C. *et al.*: 7-Hydroxymethyl chlorophyll *a* reductase functions in metabolic channeling of chlorophyll breakdown intermediates during leaf senescence. – Biochem. Biophys. Res. Commun. **430**: 32-37, 2013.
Sato Y., Morita R., Katsuma S. *et al.*: Two short-chain dehydrogenase/reductases, NON-YELLOW COLORING1 and NYC1-LIKE, are required for chlorophyll *b* and light-harvesting complex II degradation during senescence in rice. – Plant J. **57**: 120-131, 2009.
Spano G., Fonzo N.D., Perrotta C. *et al.*: Physiological characterization of "stay green" mutants in durum wheat. – J. Exp. Bot. **54**: 1415-1420, 2003.
Standfuss J., Terwisscha van Scheltinga A.C., Lamborghini M., Kühlbrandt W.: Mechanisms of photoprotection and non-photochemical quenching in pea light-harvesting complex at 2.5 A resolution. – EMBO J. **24**: 919-928, 2005.
Sunoj V.S.J., Shroyer K.J., Jagadish S.V.K., Prasad P.V.V.: Diurnal temperature amplitude alters physiological and growth response of maize (*Zea mays* L.) during the vegetative stage. – Environ. Exp. Bot. **130**: 113-121, 2016.
Thomas H., Howarth C.J.: Five ways to stay green. – J. Exp. Bot. **51**: 329-337, 2000.
Tian F.X., Gong J.F., Wang G.P. *et al.*: Improved drought resistance in a wheat stay-green mutant *tasg1* under field conditions. – Biol. Plantarum **56**: 509-515, 2012.
Tian F.X., Gong J.F., Zhang J. *et al.*: Enhanced stability of thylakoid membrane proteins and antioxidant competence contribute to drought stress resistance in the *tasg1* wheat stay-green mutant. – J. Exp. Bot. **64**: 1509-1520, 2013.
Wang F.B., Huang F.D., Cheng F.M. *et al.*: [Photosynthesis and chloroplast ultra-structure characteristics of flag leaves for a premature senescence rice mutant.] – Acta Agron. Sin. **38**: 871-879, 2012. [In Chinese] doi: 10.3724/SP.J.1006.2012.00871.
Wang W.Q., Hao Q.Q., Tian F.X. *et al.*: Cytokinin-regulated sucrose metabolism in stay-green wheat phenotype. – PLoS ONE **11**: e0161351, 2016.
Yoo S.C., Cho S.H., Zhang H. *et al.*: Quantitative trait loci associated with functional stay-green *SNU-SG1* in rice. – Mol. Cells **24**: 83-94, 2007.
Zheng H.J., Wu A.Z., Zheng C.C. *et al.*: QTL mapping of maize (*Zea mays*) stay-green traits and their relationship to yield. – Plant Breeding **128**: 54-62, 2009.